Environ. Sci. Technol. **2005**, *39,* 4180−4188

Model Demonstrating the Potential for Coupled Nitrification Denitrification in Soil Aggregates

ARIE KREMEN,* JACOB BEAR, URI SHAVIT, AND AVI SHAVIV

The Faculty of Civil and Environmental Engineering, Technion—Israel Institute of Technology, Haifa, Israel

A model of reactive, multi-species diffusion has been developed to describe N transformations in spherical soil aggregates, emphasizing the effects of irrigation with reclaimed wastewater. Oxygen demand for respiratory activity has been shown to promote the establishment of anaerobic conditions. Aggregate size and soil respiration rate were identified as the most significant parameters governing the existence and extent of the anaerobic volume in aggregates. The inclusion of kinetic models describing mineralization, nitrification, and denitrification facilitated the investigation of coupled nitrification/denitrification (CND), subject to O_2 availability. N-transformations are shown to be affected by effluent-borne NH_4^+−N content, in addition to elevated BOD and pH levels. Their incremental contribution to O_2 availability has been found to be secondary to respiratory activity. At the aggregate level, significant differences between apparent and gross rates of N-transformations were predicted (e.g., NH_4^+ oxidation and N_2 formation), resulting from diffusive constraints due to aggregate size. With increasing anaerobic volume, the effective nitrification rate determined at the aggregates level decreases until its contribution to nitrification is negligible. It was found that the nitrification process was predominantly limited to aggregates <0.25 cm. Assuming that nitrification is the main source for NO_3^- formation, denitrification efficiency is predicted to peak in medium-sized aggregates, where aerobic and anaerobic conditions coexist, supporting CND. In effluent-irrigated soils, the predicted NO_2^- formation rate in small aggregates is enhanced when compared to freshwater-irrigated soils. The difference vanishes with increasing aggregate size as anaerobic NO_2^- consumption exceeds aerobic NO_2^- formation due to the coupling of nitrification and denitrification.

1. Introduction

Irrigation with reclaimed wastewater, henceforth referred to as effluent, is widely employed in arid and semi-arid climates in an effort to optimize scarce freshwater resources. Effluent, generally characterized by elevated pH values, often contains organic matter (i.e., COD and BOD), plant macronutrients, including organic and mineral nitrogen, and miscellaneous pollutants and pathogens (*1*, *2*). Effluent application has been shown to increase soil pH, enhance NH_3 volatilization, augment the soil organic matter pool, and enhance nitrification (*3*−*6*). Decomposition of effluent-borne organic matter reduces the O_2 availability throughout the soil profile and has been linked to an increase in the production of gaseous N intermediaries during nitrification (*7*, *8*) and to an increase in the denitrification potential. The elevated sodium content of effluent has been shown to cause swelling and dispersion of the soil clay fraction, resulting in decreased hydraulic conductivity, thus impeding drainage and soil aeration (*9*−*11*). Although denitrification requires anaerobic conditions, it has been observed in well-aerated structured soils, where its occurrence has been linked to the decomposition of particulate organic matter (*12*) and to the development of anaerobic conditions in hotspots or soil aggregates (*5*, *13*, *14*).

Greenwood (*15*) and Currie (*16*) have shown experimentally and by mathematical analysis that porous soil aggregates may develop and sustain anaerobic activity. They introduced the following assumptions: (i) soil aggregates may be approximated as spheres of an equivalent radius (r_{agg}); (ii) aggregates will remain water saturated even after the inter-aggregate pores have drained; (iii) soil respiration occurs within aggregates and is the sole, homogeneously distributed oxygen sink; (iv) O_2 is abundant in the macropores; and (v) mass transfer between the macropores and the aggregates occurs by diffusion only. According to this model, soil respiration will result in an O_2 jump between the macropore and the aggregate. Anaerobic conditions will develop whenever the rate of O_2 consumption exceed the rate of O_2 diffusion into the aggregate.

This conceptual model has been described by the reactive diffusion equation, in which soil respiration (i.e., mineralization of soil organic matter) is described by zero-order kinetics (*15*). Assuming steady-state conditions, the critical radius of an aggregate (r_c) with respect to O_2 availability can be defined. Aggregates with radii larger than r_c will develop anaerobic zones, while O_2 availability will be unlimited to those with radii smaller than r_c. This model has been adopted to calculate the extent of anaerobic zones in a soil with log-normally distributed aggregate sizes, showing that the anaerobic volumetric fraction (AVF) of spherical aggregates increases with depth, depending on size distribution parameters and inter-aggregate porosity (*17*). The effect of different aggregate shapes on these results have been shown to be negligible as compared with other sources of errors in this analysis (*18*).

Arah and Smith extended Smith's model to include equations that describe steady-state transport and reduction of nitrate (NO_3^-), estimating the net denitrification rate (*17*, *19*). Their model showed that NO_3^- reduction was controlled by diffusive constraints, and they concluded that aggregates of intermediate sizes may be more efficient denitrifiers than larger ones. Myrold and Tiedje studied transient denitrification in aggregates subject to limited organic carbon supply, employing Michaelis−Menten kinetics. They found that carbon availability, rather than NO_3^-, limited the denitrification rates in the soils under investigation (*20*). McConnaughey and Bouldin (*21*) developed a model of transient denitrification in aggregates, assuming that diffusion of N species was possible throughout the saturated soil, while the reduction of N species occurred only in the anaerobic region. In their model, anaerobic conditions develop as a result of soil respiration and are balanced by O_2 diffusion from the intra-aggregate fluid in the pore space. Four types of reaction terms describing denitrification kinetics were considered. Their results indicated that a dual Michaelis−Menten expression, regulating the reduction rate based on NO_3^- and

* Corresponding author present address: Dept. of Environmental Sciences, Rutgers—The State University of New Jersey, 14 College Farm Rd., New Brunswick, NJ 08901-8551; telephone: (732)406-3205; fax: (732)932-8644; e-mail: arie@kremen.org.

10.1021/es048304z CCC: $30.25

Published on Web 04/26/2005

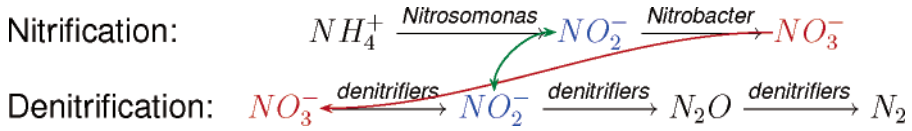

FIGURE 1. Coupled nitrification denitrification (CND) pathway, in which NO_2^- and NO_3^- derived from nitrification are directly and immediately available for denitrification.

carbon availability, as proposed by Bowman and Focht (*22*), came closest to correctly describing N_2O fluxes and the N_2/N_2O ratio. In all of the previous models, NO_3^- is assumed to be readily available and thus not limiting denitrification. However, in fertilized or effluent-irrigated soils, organic and ammoniacal nitrogen are present in addition to NO_3^-. Barring prior mineralization and nitrification, NO_3^- availability may prove to affect the occurrence of denitrification. Nevertheless, NH_4^+ oxidation in the aerobic regions of aggregates will increase NO_3^-availability, thus decreasing the potential for a limited NO_3^-supply to control the rate of denitrification, assuming anaerobic conditions develop. Under such circumstances, NO_3^- derived from nitrification would be directly and immediately available for denitrification, resulting in coupled nitrification/denitrification (CND) (Figure 1). CND is mentioned here because it is often confused with nitrifier denitrification; however, it is not a separate process (*23*). The term is used to stress that NO_2^- or NO_3^- produced during nitrification can be utilized by denitrifiers. This coupling can take place in soils where favorable conditions for both nitrification and denitrification are present in neighboring microhabitats. CND plays an important role in the removal of nitrogenous compounds in wastewater treatment, N transformations in sediments, and possibly in agricultural soils (*24*−*26*).

Kinetic descriptions of biochemical reactions are frequently coupled to mass balance equations in an effort to describe reactive miscible displacement in porous media (*27*). A commonly implied assumption is that kinetic models describe microscopic (i.e., gross or "true") reaction rates. This assumption is required for the kinetic model to be consistent with the microscopic formulation of solute transport, which averages intrinsic properties over a suitable representative elementary volume (*28*). However, diffusive constraints restrict O_2 and substrate availability, and concomitant reactions affect reaction rates that are determined on soil samples, which retain their structural integrity. This results in macroscopic (i.e., "apparent" or net) reaction rates, which do not reflect the soil specific reaction rate. Based on differential degradation rates measured in artificial dual-porosity soil columns, a strong correlation between soil structure and microbial activity has been deduced (*29*).

We suggest that diffusive constraints play an important role in explaining the discrepancy between gross and net reaction rates and provide a better insight to N-transformations under effluent irrigation. A multi-species, reactive diffusion model containing kinetic descriptions for soil respiration, mineralization of organic C contained in effluents (BOD), pH changes, nitrification, and denitrification is presented to study CND in the O_2 and substrate-limited aggregate domain and to demonstrate the effect of soil structure on kinetic coefficients. Specifically, the proposed model was employed to (i) determine O_2 availability in aggregates subjected to O_2-consuming processes, (ii) demonstrate the models' capabilities to estimate net reaction rates from microscopic (gross) rate coefficients, and (iii) characterize CND in aggregates particularly under irrigation with reclaimed effluent.

2. Model Development

A structured soil may be visualized as an assembly of porous aggregates of various shapes and sizes. The total void space of such soil is divided into an inter-aggregate void space (macropores), comprised of larger pores between the aggregates, and an intra-aggregate void space, comprised of small pores within the soil aggregates (micropores). Although aggregates have complex shapes and their sizes are commonly log-normally distributed (*30*−*32*), we assume that aggregates may be approximated as spheres with an equivalent radius. Soil properties and microorganism populations are assumed to be homogeneously distributed within the aggregate (*33*). Water is mobile in the macropores, while aggregates are assumed always to remain saturated, with essentially immobile water. Solute movement in the macropores is governed by reactive, convective−dispersive transport phenomena, while mass transport across the micropore/macropore interface and within the aggregates is only by diffusion.

The proposed model has been approximated by a finite difference formulation of the governing partial differential equation (eq 10) and the appropriate boundary conditions and function relationships. The resulting code has been implemented as a FORTRAN95 computer program.

2.1. Conceptual Model. We envision the soil as composed of an assembly of spherical porous aggregates, each surrounded by a volume of pore space, which is partly occupied by soil solution and partly by soil gas. We assume that each spherical aggregate is completely surrounded by soil solution. The macropore volume in which the aggregate is suspended is assumed sufficiently large as compared to the aggregate pore volume. Since our primary interest in this paper is to investigate what happens within the soil aggregates, we shall focus on a single spherical aggregate of radius (r_{agg}) surrounded by a constant volume of soil solution (U_{cont}) of concentration c_{aq}^{γ} for every γ species. Furthermore, the value of c_{aq}^{γ} varies because of two mechanisms: (i) equilibrium of volatile components with the atmosphere and (ii) mass exchange with the spherical aggregate. Altogether we have to consider the γ species concentration along the aggregate radius ($c^{\gamma} = c^{\gamma}(r)$) and the γ species concentration in the soil solution (c_{aq}^{γ}) as variables.

We implement the above model by assuming that every single soil aggregate is submerged in a "well-mixed" volume of a soil solution in equilibrium with the ambient atmosphere. All reactions and transformations are assumed to occur within the aggregate only. Diffusion is assumed to control mass transport across the micropore/macropore interface and within the aggregate. The kinetic models of the considered reactions are described in the following subsection. Diffusive constraints together with O_2 and substrate availability are assumed to control the occurrence of N transformations. Figure 2 depicts the processes, which may occur in aggregates.

2.2. Kinetic Models of the Chemical Reactions. The model considers the following reactions and transformations: C mineralization, nitrification, and denitrification. Two pools of organic carbon are considered: (i) immobile carbon, associated with soil organic matter, and (ii) dissolved organic carbon, introduced by effluent irrigation commonly referred to as BOD or biological O_2 demand. A three species, parent−child kinetic model that describes nitrification and a set of sequential dual Michaelis−Menten equations are employed to describe denitrification, utilizing native soil organic C as an alternative electron donor. Changes to the soil solution pH system are described by ionic mass transfer. Neither the

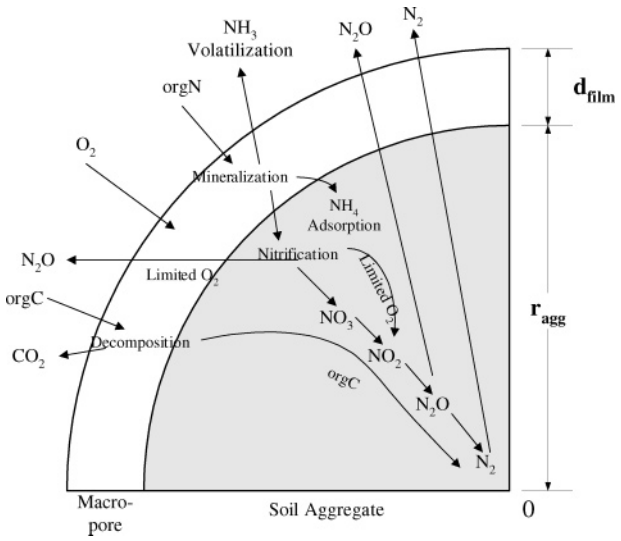

FIGURE 2. Schematic of possible C and N transformations in soil aggregates.

mineralization of the soil or effluent-borne organic N nor immobilization is considered in this version of the model. We introduce the following notation to denote the rate of change in the concentration of a γ-component consumed or produced in any process (prc):

$$R^{\gamma}|_{\text{prc}} \equiv \left.\frac{\mathrm{d}c^{\gamma}}{\mathrm{d}t}\right|_{\text{prc}} \quad \text{prc} = \text{resp, BOD, nit, denit} \qquad (1)$$

designating soil respiration (resp), biological oxygen demand (BOD), nitrification (nit), and denitrification (denit), respectively.

2.2.1. C Mineralization. Carbon mineralization occurs under aerobic conditions, and we assume that the mass of mineral C produced equals that of organic consumed C (orgC). Furthermore, during the mineralization of orgC the rate of H^+ production is assumed to be equal to that of O_2 consumption.

Soil Organic Matter. Soil respiration is the mineralization of immobile orgC, usually associated with the decomposition of roots, soil microorganisms, and soil organic matter. A zero-order kinetic model commonly describes O_2 demand for the degradation of soil organic matter. The rate of O_2 consumption in the process of soil respiration is given by

$$R^{\text{O}_2}|_{\text{resp}} = -\begin{cases} k_{\text{soilC}} & c^{\text{O}_2} > 0 \\ 0 & c^{\text{O}_2} = 0 \end{cases} \qquad (2)$$

where k_{soilC} is the soil respiration rate coefficient and c^{O_2} is the microscopic O_2 concentration (i.e., at points within the aggregate soil solution). Values cited in the literature for k_{soilC} vary widely and depend heavily on soil conditions, cultivation, cropping practices, and environmental factors, mainly temperature. A value often reported in the literature for soil respiration rates at the soil profile level is about $\text{p}K_{\text{soilC}} = 7$ (*34*−*36*), where $\text{p}K_{\text{soilC}} = -\log(k_{\text{soilC}})$.

Dissolved Organic Carbon. Dissolved organic carbon may be introduced into the soil during effluent irrigation; it is expressed as BOD. The rate of O_2 consumption is commonly described by a modified first-order kinetics, expressed as

$$R^{\text{O}_2}|_{\text{BOD}} = -k_{\text{BOD}}(L_{\text{BOD}} - c^{\text{BOD}}) \qquad (3)$$

where k_{BOD} is the BOD mineralization rate coefficient and L_{BOD} is the dissolved organic C (i.e., BOD) pool (*37*).

2.2.2. Nitrification. Nitrification is the oxidation of ammonium (NH_4^+) to NO_3^- via NO_2^- and possibly N_2O by autotrophous organisms:

$$\text{NH}_4^+ \xrightarrow[k_{\text{NH}_4^+}]{\text{nitrosomonas}} \text{NO}_2^- \xrightarrow[k_{\text{NO}_3^-}]{\text{nitrobacter}} \text{NO}_3^- \qquad (4)$$

Based on experimental results obtained by Master et al. (*38*, *39*), a three species kinetic model has been proposed. Several researchers have successfully described the rate of NH_4^+ oxidation, which is the first step of nitrification, by employing the first-order kinetics (*39*−*41*):

$$R^{\text{NH}_4^+}|_{\text{nit}} = -k_{\text{NH}_4^+} c^{\text{NH}_4^+} \qquad (5)$$

Similarly, the rate of NO_3^- production can be described by a first-order kinetics, where the nitrification intermediary (NO_2^-) serves as the substrate:

$$R^{\text{NO}_3^-}|_{\text{nit}} = k_{\text{NO}_3^-} c^{\text{NO}_2^-} \qquad (6)$$

Thus, the rate of NO_2^- formation is the difference between NO_2^- production, $R^{\text{NO}_2^-}|_{\text{nit}} = -R^{\text{NH}_4^+}|_{\text{nit}}$, and NO_3^- appearance, i.e.,

$$R^{\text{NO}_2^-}|_{\text{nit}} = k_{\text{NH}_4^+} c^{\text{NH}_4^+} - k_{\text{NO}_3^-} c^{\text{NO}_2^-} \qquad (7)$$

Stevens et al. (*42*) suggested that NO_2^- oxidation is inhibited by the presence of NH_3, which is more likely to be enhanced under effluent irrigation due to its NH_4^+ content and the elevated pH value.

Thus, based on the suggestion of Stevens et al. (*42*), enhanced NO_2^- accumulation would be expected in effluent-irrigated soils. Analysis of experimental data collected by Master validates Stevens et al.'s assumptions, as NO_2^- oxidation in freshwater-irrigated soils occurs approximately 3−5 times faster than in effluent irrigated soils. Venterea and Rolston have shown that NO_2^- build-up is linked to pH effects (*43*, *44*), which may dynamically affect nitrification kinetics. However, as the soils used in the underlaying investigation are characterized by high clay contents and strong pH buffer capacities, the dynamic feedback of the pH value on nitrification has not been considered here. Instead irrigation water quality specific, constant kinetic parameters, reflecting the effect of the pH value as established in ^{15}N incubation experiments were used (*38*, *39*).

The rate of O_2 consumption is assumed to be equal to the combined rates of NH_4^+ and NO_2^- oxidation. Nitrification ceases when the concentration of O_2 drops below a threshold value ($c_{\text{Th}}^{\text{O}_2}$). The rate of proton release is assumed to be twice that of the rate of NH_4^+ oxidation, thus causing a decrease in the solution pH.

2.2.3. Denitrification. Denitrification occurs when the concentration of O_2 drops below the threshold value ($c_{\text{Th}}^{\text{O}_2}$). Dissolved oxygen (DO) threshold concentrations reported in the literature range between 3.5 and 5 of the saturated O_2 concentration (*45*, *46*). During denitrification, NO_3^- or oxides derived from it serve as terminal electron acceptors for respiratory electron transport during the oxidation of the organic substrate, and more reduced N oxides or N_2 evolve. The dissimilatory reduction of NO_3^- releases N_2 into the soil solution and eventually into the atmosphere via soil gas. In the present model, the considered denitrification pathway is

$$\text{NO}_3^- \rightarrow \text{NO}_2^- \rightarrow \text{N}_2\text{O} \rightarrow \text{N}_2 \qquad (8)$$

On the basis of work by Bowman and Focht, the kinetic formulation for NO_3^- reduction is, usually, described by a

set of differential, dual Michaelis−Menten expressions (*22*):

$$R^{NO_3^-}|_{denit} = -V\frac{c^{NO_3^-}}{\lambda_{NO_3^-} + c^{NO_3^-}} \quad (9a)$$

$$R^{NO_2^-}|_{denit} = V\left(\frac{c^{NO_3^-}}{\lambda_{NO_3^-} + c^{NO_3^-}} - \frac{c^{NO_2^-}}{\lambda_{NO_2^-} + c^{NO_2^-}}\right) \quad (9b)$$

$$R^{N_2O}|_{denit} = V\left(\frac{c^{NO_2^-}}{\lambda_{NO_2^-} + c^{NO_2^-}} - \frac{c^{N_2O}}{\lambda_{N_2O} + c^{N_2O}}\right) \quad (9c)$$

$$R^{N_2}|_{denit} = V\frac{c^{N_2O}}{\lambda_{N_2O} + c^{N_2O}} \quad (9d)$$

where V, denoting the maximum reaction rate under unlimited substrate supply, and λ_γ are Michaelis−Menten parameters. Assuming that formaldehyde (CH_2O) or a similar compound is the alternative electron donor under anaerobic conditions, the rate of OH^- production can be shown to be equal to that of NO_2^- reduction, thus effectively increasing the solution pH.

Although Bowman and Focht suggested a Michaelis−Menten-type term to determine V, a constant value may be employed, especially if the organic C availability is nonlimiting. In agricultural soils subject to effluent irrigation, C availability in microsites is assumed to be always unlimited, and thus the use of an unmodified reaction rate (V) is justified (*21*, *47*).

2.3. Mathematical Model. Multi-species reactive diffusion describing N transformations under transient conditions within a spherical soil aggregate of radius (r_{agg}) can be described by the mass balance equation for every γ-component present within the aggregate:

$$R_f^\gamma \frac{\partial c^\gamma}{\partial t} = \mathscr{D}_{agg}^{*,\gamma}\nabla^2 c^\gamma + \sum_{(prc)} R^\gamma|_{prc} \quad (10)$$

$$\gamma = NH_4^+, NO_2^-, NO_3^-, N_2O, N_2, O_2, \text{and } H^+$$

where c^γ is the inter-aggregate pore soil solution concentration of a γ-component, R_f^γ is the retardation factor for a γ-component, and $\mathscr{D}_{agg}^{*,\gamma}$ is the γ-component diffusion coefficient in the aggregate micropores. As a component may participate in several reactions, its respective production and consumption rates ($R^\gamma|_{prc}$) are expressed by the last term on the right-hand side of eq 10, its net rate of change.

For the two cationic species NH_4^+ and H^+, the retardation factors $R_f^{NH_4^+}$ and $R_f^{H^+}$, respectively, describing the effect of cation adsorption to the soil clay fraction are expressed by

$$R_f^{NH_4^+} = 1 + \frac{\rho_{agg}k_d^{NH_4^+}}{\phi_{agg}} \text{ and } R_f^{H^+} = 1 + \frac{\rho_{agg}\beta_H}{\phi_{agg}}\frac{\log e}{c^{H^+}}, \quad (11)$$

where ρ_{agg} is the aggregate bulk density and θ_{agg} is the aggregate water content. As aggregates are assumed to *always* remain saturated, $\theta_{agg} \equiv \phi_{agg} = \text{const}$, where the latter denotes the aggregate porosity; $k_d^{NH_4^+}$ and β_H are the linear sorption coefficient and soil buffer capacity (*48*, *49*), respectively. The aggregate is assumed to be homogeneous and isotropic, thus symmetry with respect to the origin of the spherical aggregate may be employed to simplify the mathematical description.

2.3.1. Boundary Conditions. Linked by the components' production and consumption rate terms, a system of partial differential equations is defined by eq 10, which has to be solved simultaneously for all γ subject to appropriate initial and boundary conditions. The latter have to be specified on the external spherical surface of the aggregate. The boundary conditions that have to be prescribed at the aggregate perimeter ($r = r_{agg}$) depend on whether the γ species is volatile or nonvolatile. As the soil solution surrounding the aggregate is assumed to be exposed to the ambient atmosphere, the concentrations of volatile species in the soil solution are in equilibrium with the atmosphere.

A Dirichlet or a "no jump" boundary condition describes the continuous component concentration across the aggregate's perimeter, i.e.

$$c^\gamma|_{r=r_{agg}} = c_{aq}^\gamma \quad (12)$$

where c_{aq}^γ is the soil solution γ-component concentration in equilibrium with the atmosphere. For a volatile species, the solution concentration is given by

$$c_{aq}^\gamma = p_g^\gamma k_H^\gamma \equiv \text{const}^\gamma \quad \gamma = O_2, N_2O, \text{and } N_2 \quad (13)$$

where p_g^γ and k_H^γ are the atmospheric partial pressure and Henry's law coefficient, respectively.

The considered γ species may accumulate or be depleted in the soil solution within U_{cont}. Their mass transfer across the aggregate boundary is described by the diffusive flux at $r = r_{agg}$, which is formulated employing a Fickian-type term. The resulting boundary condition for the remaining, nonvolatile species is given by

$$\frac{\partial c_{aq}^\gamma}{\partial t} = -\mathscr{D}_{agg}^{*,\gamma}\frac{A_{agg}}{U_{cont}}\left.\frac{\partial c^\gamma}{\partial r}\right|_{r=r_{agg}} \quad (14)$$

$$\gamma = NH_4^+, NO_2^-, \text{and } NO_3^-$$

where A_{agg} is the surface area of an aggregate of radius r_{agg}, and U_{cont} is the volume of the soil solution surrounding the aggregate (i.e., macropore). Solving eqs 10 and 14 simultaneously yields the aggregate concentration profile and the soil solution composition for each of the γ-components.

2.3.2. Initial Conditions. Oxygen availability has a significant effect on the reactions occurring within an aggregate. Assuming that the sole O_2-consuming process is soil respiration, steady-state O_2 concentration profiles may be derived from eq 10. Currie determined the critical radius of a spherical aggregate:

$$r_c = \sqrt{\frac{6\mathscr{D}_{agg}^{*,O_2}c_{aq}^{O_2}}{k_{soilC}}} \quad (15)$$

as the radius of the largest aggregate, which may remain completely aerobic for given values of the intra-aggregate O_2 diffusion coefficient, macropore O_2 concentration, and soil respiration rate (*16*). Initial O_2 concentration profiles have been determined from the steady-state O_2 solution of eq 10:

$$c^{O_2}(r, 0) = \begin{cases} \begin{cases} \dfrac{c_{aq}^{O_2}}{(r_{agg} - r_c)^2}(r - r_c)^2 & r \geq r_c \\ 0 & r_{agg} > r_c \end{cases} & r > r_c \\ \dfrac{k_{soilC}}{6\mathscr{D}_{agg}^{*,O_2}}(r^2 - {r_{agg}}^2) + c_{aq}^{O_2} & r_{agg} \leq r_c \end{cases} \quad (16)$$

The initial aggregate NH_4^+ content is set to zero, i.e. $c^{NH_4^+}(r, 0) = 0$. The initial NH_4^+ concentration in the soil solution surrounding the aggregate is set to 100 ppm. In the simulations, the volumetric ratio between the volumes was set to 5:1. The initial overall pH was set to 7.0. To facilitate

the investigation of CND in aggregates, the initial concentrations of the remaining N species within the aggregate and the soil solution were set to zero.

3. Simulations and Results

The conceptual and mathematical models described in the previous section were applied to the study of CND in spherical soil aggregates. The existence and extent of AVF were simulated for a wide range of radii and soil respiration rates. The incremental effects of concomitant O_2-consuming processes were evaluated for ranges of NH_4^+ and BOD concentrations covering freshwater effluent and untreated wastewater. Diffusive constraints were shown to affect reaction rates, determined macroscopically at the aggregate level, resulting in apparent (net) rates. The effect of diffusive constraints was investigated by comparing apparent and gross nitrification rates, in aggregates of varying sizes. The occurrence of CND was evaluated over a range of macropore solution compositions, radii, and respiration rates. The objective was to identify the parameters having the greatest influence on N transformations.

The soil aggregate model is rather parameter intensive, requiring diffusion rates, reaction rate coefficients, and soil properties. Wherever possible, preference was given to post-processing data obtained experimentally (*38*, *39*, *50*, *51*) (e.g., nitrification kinetics and soil properties). If relevant data were not easily obtainable, published values have been used. Sensitivity analyses have been performed for parameters to determine the stability of the results shown.

3.1. Oxygen Availability. Oxygen availability varying along the aggregate radius is the major environmental factor affecting the fate of N transformations. The O_2-consuming processes considered for this work are dissolved organic C, BOD, mineralization, soil respiration, and nitrification. To quantify the affect of each process on O_2 availability, two indices have been formulated: (i) AVF, which expresses the anaerobic volumetric fraction of an aggregate, and (ii) DOS, volumetric averaged decrease from O_2 saturation. The AVF is defined as the fraction of the aggregate volume where the O_2 concentration is below the threshold value $c_{Th}^{O_2}$. The decrease from O_2 saturation (DOS) describes the marginal change in O_2 availability, applied to processes that are not sufficiently strong to induce anaerobic conditions.

3.1.1. Soil Respiration. Using eq 15, the steady-state anaerobic volume can be solved analytically. The existence and extent of anaerobic volumes were determined for aggregate radii between 0.125 and 2.125 cm and soil respiration rates ranging from $pK_{soilC} = 5.0-9.0$ (Figure 3).

Assuming that the O_2 diffusion rate remains constant and that the macropore O_2 concentration remains saturated, the calculated equi-AVF lines are described in Figure 3 as curves whose slopes are determined by aggregate radius and the soil respiration rate: the anaerobic volume increasing parabolically with radius and exponentially with soil respiration rate. For the median respiration rate of $pK_{soilC} = 7.0$, virtually no anaerobic conditions develop in aggregates with radii smaller than 0.75 cm. For increasing radii, the AVF increases steadily until approximately 60% of the aggregate becomes anaerobic. For respiration rates lower than about $pK_{soilC} = 7.75$, no significant anaerobic zones develop at all radii. At very high respiration rates, $pK_{soilC} < 6$, all but the smallest aggregates considered ($r_{agg} < 0.25$ cm) develop anaerobic zones, with those having radii larger than 0.75 cm establishing AVFs in excess of 80%.

3.1.2. Mineralization and Nitrification. The effect of BOD and nitrification on aggregate O_2 availability was investigated, assuming that no soil respiration occurs (i.e., $K_{soilC} = 0$). Results are expressed in terms of the average decrease from O_2-saturated conditions, DOS. Three major factors may affect aggregate O_2 availability under either process: (i) aggregate size, (ii) microscopic reaction rate, and (iii) macropore substrate availability. In the following simulations, the macropore substrate content was kept constant (i.e., $c_{aq}^{\gamma} = \text{const}$). A sensitivity analysis was performed for macropore and BOD concentrations representing a wide range from freshwater to raw wastewater compositions and for aggregate radii between 0.125 and 2.125 cm.

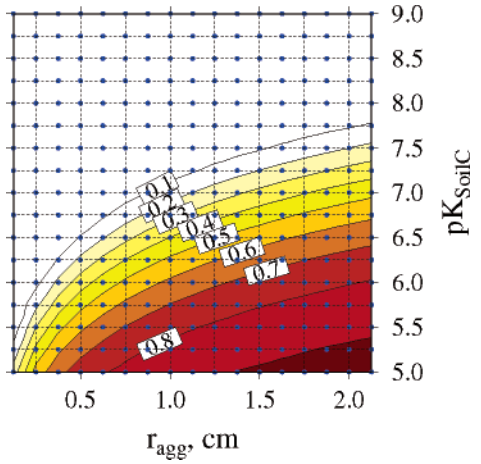

FIGURE 3. Calculated steady-state anaerobic volume fractions (AVF) in soil aggregates as functions of aggregate radius (r_{agg}) and soil respiration rate (pK_{soilC}), assuming unlimited macropore O_2 availability.

In incubation experiments, Master determined the first-order rate coefficient for oxidation ($k_{NH_4^+}$) in aggregated clay soils to be in the range between 0.4 and 0.6 1/d (*39*). Nitrification rates were found to depend on soil types. BOD rates ranged between 0.1 and 0.3 1/d. The rate of O_2 demand due to nitrification is insufficient to produce anaerobic conditions. Even under high macropore NH_4^+ concentrations, $c_{aq}^{NH_4^+} > 100$ ppm, and the average aggregate O_2 concentration drops only by about 80 (Figure 4a) insufficient for anaerobic conditions; the latter require a decrease in O_2 concentration of about 95%. Similarly, the BOD was found to be insufficient to cause the development of anaerobic conditions. Its effect on aggregate O_2 availability is marginal in aggregates with $r_{agg} < 1.5$ cm and becomes significant only for macropore dissolved organic C concentrations in excess of 50 ppm (Figure 4b). Even though either process by itself does not induce anaerobic conditions, together they contribute to the overall O_2 demand and will contribute to an increase to the anaerobic region resulting from soil respiration.

3.2. Microscopic versus Macroscopic Kinetics of Ammonium Oxidation. The microscopic mass balance equation within the aggregate (eq 10) includes the reaction rate within the domain, assuming that substrate and O_2 availability are not limiting factors. However, at the aggregate level, transport phenomena, concomitant N transformations, and reactions will affect substrate availability. By determining the change in NH_4^+ mass present in the model domain and fitting the data to a first-order kinetic model curve, the macroscopic or apparent (i.e., net) ammonium oxidation rate was determined. In all cases, correlation coefficients were close to unity. Simulations were performed for aggregate radii ranging from 0.05 to 3.0 cm. Sensitivity to O_2 availability was evaluated by applying different soil respiration rates, $pK_{soilC} = 7.0$, 7.5, and 8.0, and by comparison to a hypothetic scenario under which $K_{soilC} = 0$. The microscopic value for the rate coefficient was obtained from batch incubation experiments, conducted by Master, using labeled NH_4^+, $k_{NH_4^+} = 0.6$ 1/d (*39*). The resulting, calculated apparent nitrification rates were normalized with respect to the microscopic rate to yield the relative NH_4^+ oxidation rate (Figure 5).

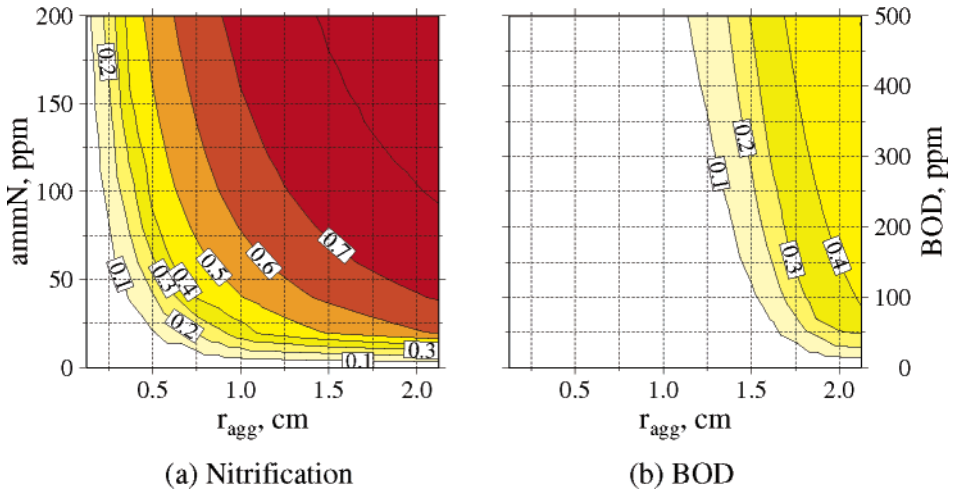

FIGURE 4. Average percentage drop in relationship to O_2-saturated conditions in aggregates of varying sizes and exposed to a range of macropore (a) ammonical N (ammN) and (b) BOD concentrations, assuming a nitrification rate of $k_{NH_4^+} = 0.6$ 1/d, and a dissolved organic carbon mineralization rate of $k_{BOD} = 0.3$ 1/d.

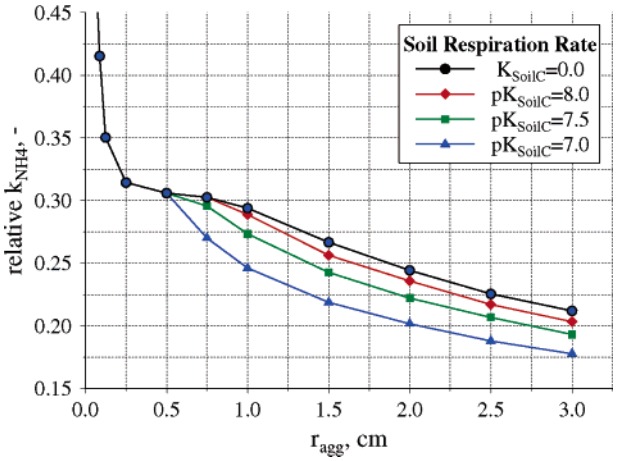

FIGURE 5. Relative NH_4^+ oxidation rates resulting from solving eq 10 with a microscopic rate $k_{NH_4^+} = 0.6$ 1/d.

The results indicate that the relative nitrification rate decreases with aggregate size and with limited O_2 availability and ranges between 17% for the largest aggregates to about 60% for the smallest ones considered (results not shown). For aggregates smaller than approximately 0.5 cm, O_2 availability is nonlimiting (Figure 5). However, diffusive transport exerts a strong influence on the relative nitrification rate, which increases rapidly for the smallest aggregates, from 30% to about 60%. Increasing the respiration rates causes an additional reduction in the relative nitrification rate for aggregates larger than 0.5 cm. It should be noted that the focus in this study is on physical constraints that induce the discrepancy between apparent and gross transformation rates, whereas the consideration of additional microbial processes (e.g., N-mineralization or immobilization) may further complicate the system.

3.3. Coupled Nitrification/Denitrification. 3.3.1. Nitrate and Di-nitrogen Formation. Simulation results presented in the previous subsections show that soil respiration, together with aggregate size, are the two major parameters determining the existence and extent of anaerobic zones in aggregates. Assuming the development of anaerobic conditions and the availability of NH_4^+, the prerequisites for coupled nitrification/denitrification to occur in aggregates are met. In the subsequent set of simulations, the occurrence of CND in aggregates subject to O_2 availability and over a range of radii has been characterized. In lieu of experimental denitrification data, values for kinetic coefficients suggested by McConnaughey and Bouldin were used, namely, $\lambda_{NO_3^-} = 0.63$ mol N/m^3. Betlach and Tiedje and McConnaughey and Bouldin used identical values for NO_3^- and NO_2^- reduction, when described by the Michaelis−Menten kinetics (*52*, *53*). The value for N_2O reduction was given as $\lambda_{N_2O} = 3.6 \times 10^{-2}$ mol N/m^3. Figure 6 shows the normalized amounts of NO_3^- and N_2 produced after 24 h, respectively. As nitrification requires aerobic conditions, significant NH_4^+ oxidation takes place in aggregates with $r_{agg} < 0.5$ cm, under soil respiration rates with $pK_{soilC} > 6.5$. Such aggregates were identified as having the greatest relative nitrification rate. In aggregates with radii greater than approximately 0.5 cm, nitrification is progressively inhibited by extensive anaerobic zones (Figures 6a and 3), thus only relatively small amounts of NH_4^+ are oxidized. As diffusive constraints were shown to limit nitrification in large aggregates ($r_{agg} > 1.0$ cm), NO_3^- production lags behind that of smaller ones. With increasing AVFs, nitrification in aggregates becomes more restricted (i.e., the apparent nitrification rate decreases), resulting in decreased NO_3^- production (Figures 5 and 6).

Di-nitrogen (N_2) production under CND (Figure 6b) requires both the existence of anaerobic conditions and the presence of NO_3^-. Even though NO_3^- availability is nonlimiting in small aggregates and under low respiration rates, the lack of anaerobic conditions precludes reduction. In aggregates with AVF > 0.7, NO_3^- availability becomes the limiting factor, thus impeding N_2 evolution. Denitrification efficiency (i.e., the capability of aggregates to produce N_2) is the greatest in aggregates with AVFs in the range of 0.1−0.2.

3.3.2. Nitrite Formation. Nitrite is an intermediary nitrogen oxide, common to the nitrification and denitrification processes (Figure 1). Its production rate during nitrification has been shown to be dependent on the pH value of the soil solution (*42*, *54*−*56*). Studying nitrification kinetics in soils, Master has observed an increased NO_2^- accumulation in effluent-irrigated soils as compared to freshwater-irrigated ones, indicating a significant nitrite toxicity hazard to effluent irrigated crops (*38*). The analysis of his data showed that NH_4^+ oxidation is fairly insensitive to irrigation water quality; however, NO_2^- oxidation was significantly affected by the elevated pH of the effluent. Calculated NO_2^- oxidation rates are 4.35 and 1.62 1/d for freshwater and effluent, respectively.

Simulation results (Figure 7a) show that the accumulation of NO_2^- under either treatment increases rapidly to a peak value, followed by a gradual asymptotic decline. In small to medium size aggregates ($r_{agg} < 1.5$ cm), the differences between the two treatments are quite pronounced, dimin-

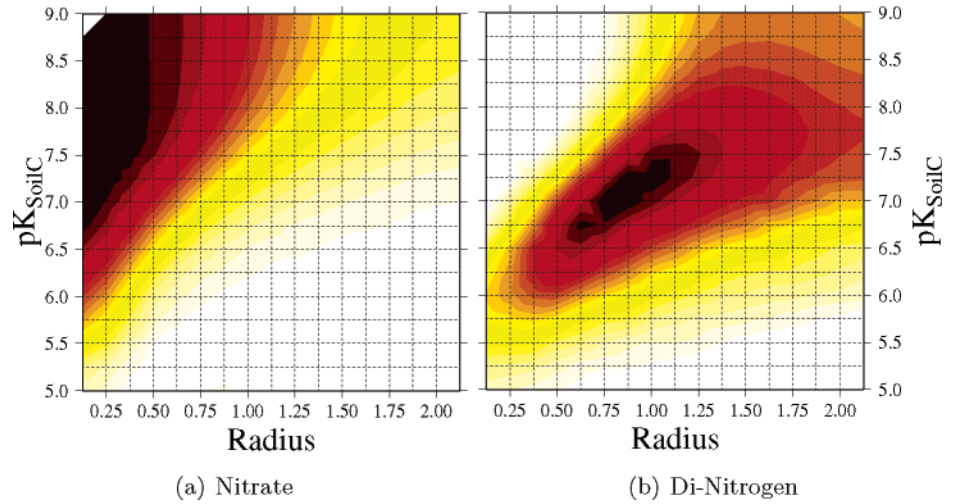

FIGURE 6. Normalized mass of NO_3^- and N_2 produced in a coupled nitrification/denitrificationsystem after 24 h. Dark colors indicate large amounts of either NO_3^- or N_2 produced, while increasingly lighter colors denote decreasing amounts.

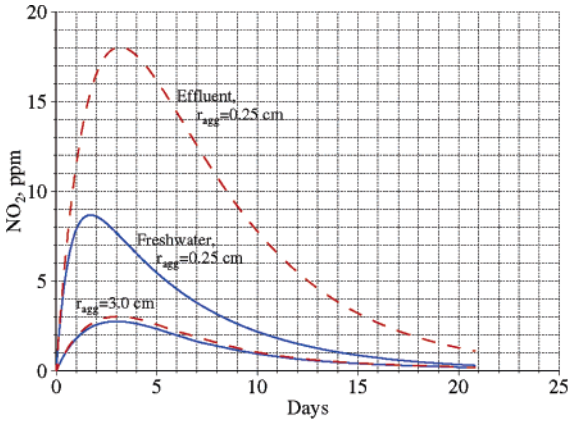

(a) NO_2^- Accumulation with for constant aggregate radii

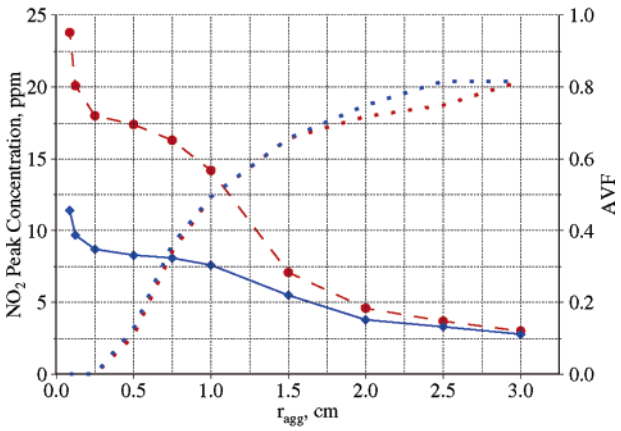

(b) NO_2^- Peak concentrations versus aggregate radii

FIGURE 7. NO_2^- appearance and peak concentrations in aggregates: $pK_{SoilC} = 7$, $k_{NH_4^+} = 0.6$ 1/d, freshwater $k_{NO_3^-} = 4.35$ 1/d, effluent $k_{NO_3^-} = 1.62$ 1/d. Freshwater: blue, solid line; effluent: red, dashed line; AVF: dotted lines.

ishing with increasing aggregate size, until they become insignificant (Figure 7b). The accumulation of NO_2^- is negatively correlated to the existence and extent of the anaerobic volume in aggregates. In aggregates smaller than $r_{agg} = 0.25$ cm, no anaerobic conditions are established, and NO_2^- accumulation is mainly affected by ammonium diffusive constraints and differences in $k_{NO_3^-}$ only. With an increase of the aggregate radius, anaerobic conditions develop and NO_2^- diffuses into the anaerobic zone, where it is rapidly reduced. As aggregate size further increases (r_{agg} > 1.5 cm), NO_2^- production becomes increasingly limited, while denitrification becomes the dominant process, rapidly reducing oxidized NH_4^+ and inducing a sharp NO_2^- gradient toward the aggregate center. Results demonstrate the importance of aggregate size in controlling the formation of nitrite in soils and particularly in effluent irrigated ones, indicating that maintaining large enough aggregates may mitigate nitrite toxicity.

4. Discussion

The existence of aggregates in structured soils is used to explain the occurrence of anaerobic processes in otherwise aerobic soils. Diffusive constraints, depending mainly on aggregate size and soil respiration rate, were shown to strongly affect O_2 availability. With increasing anaerobic volume, aggregates become less "aerobically reactive", leading to a clear differentiation between the gross and apparent reaction rates of N processes, which are sensitive to oxygen concentration. As diffusive constraints diminish in the smallest aggregates, the apparent reaction rate of NH_4^+ oxidation asymptotically approaches the gross rate, which describes the soil-specific reaction rate. The apparent reaction rate integrates over a large number of variables (e.g., concurrent processes and soil structure). Hence, experimental determination of "true" rates requires that soil samples be preprocessed to eliminate structures sufficiently large so as to impose diffusive constraints. In experimental designs that require the conservation of the soil structure, labeled substrate (e.g., $^{15}N{-}NH_4^+$ or $^{15}N{-}NO_3^-$) may be employed to prevent transport phenomena from obscuring results (*57*, *58*). Furthermore, to verify the findings of the proposed model, advanced approaches utilizing isotope dilution techniques (e.g., Müller et al.; *59*) should be utilized in experiments where N transformations are studied with aggregated soils under varying aeration and moisture conditions. One should note that mineralization is not dealt with in this model, as the main N source is assumed to be ammoniacal N, which is continuously supplied in significant amounts under effluent irrigation. As the C/N ratio in effluent irrigated soil is expected to be too low for immobilization to occur, this process has been neglected. However, mineralization and immobilization may significantly affect N-dynamics and thus induce a considerable difference between "true" (gross) and the observed (net) rates. Their impact should as well be investigated in future studies, both experimentally employing ^{15}N and in simulation models.

In the current model formulation, all reactions are assumed to occur within aggregates. However, aerobic processes are also likely to occur in the macropores, on the aggregate surfaces, or within micro-aggregates (r_{agg} < 0.03 cm) (*60*). Chenu et al. showed that nitrifying microorganisms in sandy soils are distributed across aggregates, while in clayey soils, microbial populations were concentrated on the aggregates' surface (*61*). Due to limitations of oxygen supply, results obtained in this work show that with increasing aggregate size, anaerobic conditions become prevalent within the aggregate, and nitrification occurs in the aerobic part of the aggregates, close to its surface. Thus, despite the assumption that nitrifying microorganisms are equally distributed in the aggregates, the physical constraints limit the oxidation process to small aggregates or to the aerobic regions close to the surface of the larger ones.

Ammonium nutrition is common in fertilized fields or under effluent irrigation. Its application to aggregates subject to oxygen limitations may result in CND; this may play an important role in controlling N gaseous losses and NO_2^- formation, particularly under effluent irrigation. Three effects of effluent irrigation on CND in aggregates have been evaluated: (i) increased BOD, (ii) ammonium level, and (iii) inhibition of NO_2^- formation during nitrification. BOD has been shown to only marginally affect aggregate O_2 status, unless macropore BOD content exceeds approximately 100 ppm. The effect of ammonium oxidation is more pronounced, although, within the tested range, the process significantly reduces oxygen concentration but not sufficiently to induce anaerobic conditions. When superimposed on soil respiration, it may contribute significantly to the establishment of anaerobic conditions in aggregates larger than about 1.0 cm and exposed to macropore NH_4^+ concentrations above 25 ppm. As a result, smaller aggregates will develop anaerobic conditions.

As nitrification requires aerobic conditions, significant NH_4^+ oxidation takes place in relatively small aggregates (e.g., r_{agg} < 0.5 cm), and when soil respiration rates pK_{soilC} are >6.5. Diffusive constraints and higher soil respiration limit nitrification in aggregates with r_{agg} > 1.0 cm, due to the increasing aerobic volume fraction. Di-nitrogen production under CND requires the existence of both anaerobic conditions and aerobic ones for the production of NO_3^-. Under low respiration rates, NO_3^- availability is nonlimiting in small aggregates, but the lack of anaerobic conditions precludes NO_3^- reduction. In aggregates with AVF > 0.7, NO_3^- formation becomes the limiting factor, thus impeding N_2 evolution. Denitrification is the greatest in aggregates with AVFs of about 0.1−0.2, where enough ammonium is oxidized on one hand and the anaerobic core of the aggregates is sufficiently effective for reducing the newly formed nitrate.

Nitrite accumulation in effluent-irrigated soils is known to be larger than in freshwater-irrigated soils due to the reduced rate of its oxidation to nitrate under the conditions induced by the effluent, higher pH, and ammonia concentrations. Nitrite produced during the first step of nitrification (i.e., $NH_4^+ \rightarrow NO_2^-$) may diffuse into the anaerobic region of the aggregate, pointing to an additional, alternative pathway for CND. Under such pathway, some of the NO_2^- is not oxidized to NO_3^- but is directly reduced to N_2 (Figure 1). The importance of this pathway increases with aggregate size and anaerobic volume, until nitrification becomes the rate-limiting factor for denitrification. Simulations comparing NO_2^- formation under freshwater and effluent irrigation show much larger concentrations of the ion induced by effluent irrigation in small aggregates. As the aggregates get larger, oxygen supply becomes more restricted and, with it, NO_2^- formation via nitrification, whereas its consumption by denitrification is enhanced. These effects are more pronounced with the effluent than with the freshwater and thus in large aggregates (e.g., r_{agg} > 1.5 cm) or for AVF > 0.7, NO_2^- formation is dramatically reduced and the large differences between the two types of water almost disappear.

Nitrous oxide (N_2O) appearance has been observed in field and laboratory settings during nitrification as well as during denitrification (*8*, *26*, *38*, *39*, *42*). The formation of N_2O could have been dealt with in a similar manner as NO_2^-, as yet another pathway for CND, affecting the ratio of N_2/N_2O evolved in a given system. However, due to the lack of established mechanisms and kinetic models for the evolution of N_2O during nitrification, we preferred not to analyze this option at the current stage.

Consideration of anaerobic aggregates in reactive transport models as source or sink terms closes a conceptual gap between single- and multi-porosity formulations by facilitating the description of multi-porosity domains without requiring explicit description of the boundaries between the two porous medium subdomains. The proposed model showed that coupled nitrification/denitrificationmight occur in aggregated, agricultural soils, yet with negligible contribution of larger, anaerobic aggregates to nitrification. Nevertheless, their presence facilitates the occurrence of anaerobic processes in aerobic soil profiles.

Literature Cited

(1) Feigin, A.; Feigenbaum, S.; Limoni, H. Utilization efficiency of nitrogen from sewage effluent and fertilizer applied to corn plants growing in a clay soil *J. Environ. Qual.* **1981**, *10,* 284−287.

(2) EIS2001. National Wastewater & Effluent Irrigation Survey 1998−2000. Technical Report. State of Israel, Ministry of Agriculture and Rural Development, 2001 (in Hebrew).

(3) Steenhuis, T. S.; Bubenzer, G. D.; Converse, J. C. *Ammonia Volatilization of Winter Spread Manure*; ASAE Paper 76-4514, ASAE: St. Joseph, MO, 1976.

(4) Hoff, J. D.; Nelson, D. W.; Sutton, A. L. Ammonia volatilization from liquid swine manure applied to cropland *J. Environ. Qual.* **1981**, *10* (1), 90−95.

(5) Petersen, S. O.; Nielsen, T. H.; Frostegård, A.; Olesen, T. O_2 uptake, C metabolism and denitrification associated with manure hot-spots. *Soil Biol. Biochem.* **1996**, *28* (3), 341−349.

(6) Hengnirun, S.; Barrington, S.; Prasher, S. O.; Lyew, D. Development and verification of a model simulating ammonia volatilization from soil and manure. *J. Environ. Qual.* **1999**, *28,* 108−114.

(7) Parton, W. J.; Mosier, A. R.; Ojima, D. S.; Valentine, D. W.; Schimmel, D. S.; Weier, K.; Kulmala, A. E. Generalized model for N_2 and N_2O production from nitrification and denitrification. *Global Biogeochem. Cycles* **1996**, *10*, 401−412.

(8) Venterea, R. T.; Rolston, D. E. Mechanisms and kinetics of nitric and nitrious oxide production during nitrification in agricultural soil. *Global Change Biol.* **2000**, *6,* 303−316.

(9) Vandervivre, P.; Baveye, P. Effect of bacterial extracellular polymers on the saturated hydraulic conductivity of sand columns. *Appl. Environ. Microbiol.* **1992**, *58* (5), 1690−1698.

(10) Levy, G. J.; Levin, J.; Shainberg, I. Prewetting rate and aging effects on seal formation and interrill soil erosion. *Soil Sci.* **1997**, *162,* 131−139.

(11) Moutier, M.; Shainberg, I.; Levy, G. J. Hydraulic gradient, aging and water quality effects on hydraulic conductivity of a vertisol. *Soil Sci. Soc. Am. J.* **1998**, *62,* 1488−1496.

(12) Parkin, T. B. Soil microsites as a source of denitrification. *Soil Sci. Soc. Am. J.* **1987**, *51,* 1194−1199.

(13) Rice, C. W.; Sierzega, P. E.; Tiedje, J. M.; Jacobs, L. W. Stimulated denitrification in the microenvironment of a biodegradable organic waste injected into soil. *Soil Sci. Soc. Am. J.* **1988**, *52,* 102−108.

(14) Nielsen, T. H.; Revsbech, N. P. Nitrification, denitrification and N-liberation associated with two type of organic hotspots in soil. *Soil Biol. Biochem.* **1998**, *30* (5), 611−619.

(15) Greenwood, D. J. The effect of oxygen concentration on the decomposition of organic materials in soil. *Plant Soil* **1961**, *XIV* (4), 360−376.

(16) Currie, J. A. Gaseous diffusion in the aeration of aggregated soils. *Soil Sci.* **1961**, *92,* 40−45.

(17) Smith, K. A. A model of the extent of anaerobic zones in aggregated soils and its potential application to estimates of denitrification. *Soil Sci.* **1980**, *31,* 263−277.

(18) Rappolt, C. Diffusion in Aggregated Soil. Doctoral thesis, Wageningen Agricultural University, Wageningen, The Netherlands, 1992.
(19) Arah, J. R. M.; Smith, K. A. Steady-state denitrification in aggregated soils: A mathematical model. *J. Soil Sci.* **1989**, *40,* 139−149.
(20) Myrold, D. D.; Tiedje, J. M. Diffusional constraints on denitrification in soil. *Soil Sci. Soc. Am. J.* **1985**, *49,* 651−657.
(21) McConnaughey, P. K.; Bouldin, D. R. Transient macrosite models of denitrification: I. model development. *Soil Sci. Soc. Am. J.* **1985**, *49,* 886−891.
(22) Bowman, R. A.; Focht, D. D. The influence of glucose and nitrate concentrations upon denitrification rates in sandy soil. *Soil Biol. Biochem.* **1974**, *6,* 297−301.
(23) Wrage, N.; Velthof, G. L.; Beusuchem, M. L.; Oenema, O. Role of nitrifier denitrification in the production of nitrous oxide. *Soil Biol. Biochem.* **2001**, *33* (12−13), 1723−1732.
(24) Tartakovsky, B.; Kotlar, E.; Sheintuch, M. Coupled nitrification−denitrification processes in a mixed culture of coimmobilized cells: analysis and experiment. *Chem. Eng. Sci.* **1996**, *51* (10), 2327−2336.
(25) Rust, C. M.; Aelion, C. M.; Flora, J. R. V. Control of pH during denitrification in subsurface sediment microcosmos using encapsulated phosphate buffer. *Water Res.* **2000**, *34* (5), 1447−1454.
(26) Russow, R.; Sich, I.; Neue, H. U. The formation of the trace gases NO and N_2O in soils by the coupled processes of nitrification and denitrification: results of kinetic ^{15}N tracer investigations. *Chemosphere*: *Global Change Sci.* **2000**, *2* (3−4), 359−366.
(27) Bear, J. *Hydraulics of Groundwater*; Water Resources and Environmental Engineering, McGraw-Hill Inc.: New York, 1979.
(28) Bear, J.; Bachmat, Y. *Introduction to Modeling of Transport Phenomena in Porous Media*, *Vol. 4*, *Theory and Application of Transport in Porous Media*; Kluwer Academic Publishers: Dordrecht, The Netherlands, 1990.
(29) Pivetz, B. E.; Steenhuis, T. S. Soil matrix and macropore biodegradation of 2,4-D. *J. Environ. Qual.* **1996**, *24,* 564−570.
(30) Gardner, W. R. Representation of soil aggregate size distribution by a logarithmic-normal distribution. *Am. Proc. Soil Sci. Soc.* **1956**, *20,* 151−153.
(31) Allmaras, R. R.; Burwell, R. E.; Voorhees, W. B.; Larson, W. E. Aggregate size distribution in the row zone of tillage experiments. *Am. Proc. Soil Sci. Soc.* **1965**, *29,* 645−650.
(32) Smith, K. A. Soil aeration. *Soil Sci.* **1977**, *123,* 284−291.
(33) Giménez, D.; Karmon, J. L.; Posadas, A.; Shaw, R. K. Fractal dimensions of mass estimated from intact and eroded soil aggregates. *Soil Tillage* **2002**, *64,* 165−172.
(34) Wilson, J. M.; Griffin, D. M. Water potential and the respiration of microorganisms in the soil. *Soil Biol. Biochem.* **1975**, *7,* 199−204.
(35) MacDonald, N. W.; Zak, D. R.; Pregitzer, K. S. Temperature effects on kinetics of microbial respiration and net nitrogen and sulfur mineralization. *Soil Sci. Soc. Am. J.* **1995**, *59,* 233−240.
(36) Zak, D. R.; Holmes, W. E.; MacDonald, N. W.; Pregitzer, K. S. Soil temperature, matric potential and the kinetics of microbial respiration and nitrogen mineralization. *Soil Sci. Soc. Am. J.* **1999**, *63,* 575−584.
(37) Tchobanoglous, G. *Wastewater Engineering*: *Treatment, Disposal and Reuse*, 3rd ed.; Metcalf & Eddy Inc.: Singapore, 1991.
(38) Master, Y.; Laughlin, R. J.; Shavit, U.; Stevens, R. J.; Shaviv, A. Gaseous nitrogen emissions and mineral nitrogen transformations as affected by reclaimed effluent application. *J. Environ. Qual.* **2003**, *32* (4), 1204−1211.
(39) Master, Y.; Laughlin, R. J.; Stevens, R. J.; Shaviv, A. Nitrite formation and nitrous oxide emissions as affected by reclaimed effluent application. *J. Environ. Qual.* **2004**, *33* (3), 852−860.
(40) Hagin, J.; Welte, E.; Dianati, M.; Kruh, G.; Kenig, A. *Nitrogen Dynamics Model*−*Verification and Practical Application*; Verlag Erich Goltze: Göttingen, Germany, 1984.
(41) Myrold, D. D.; Tiedje, J. M. Simultaneous estimation of several nitrogen cycle rates using ^{15}N: Theory and application. *Soil Biol. Biochem.* **1986**, *18* (6), 559−568.
(42) Stevens, R. J.; Laughlin, R. J.; Burns, L. C.; Arah, J. R. H.; Hood, R. C. Measuring the contribution of nitrification and denitrification to the flux of nitrous oxide from soil. *Soil Biol. Biochem.* **1997**, *29* (2), 39−151.
(43) Paul, W.; Domsch, K. H. Ein mathematisches modell für den nitrifikationsprozess im boden. *Arch. Microbiol.* **1972**, *87,* 77−92.
(44) Venterea, R. T.; Rolston, D. E. Mechanistic modeling of nitrite accumulation and nitrogen oxide gas emissions during nitrification. *J. Environ. Qual.* **2000**, *29*, 1741−1751.
(45) Parkin, T. B.; Tiedje, J. M. Application of a soil core method to investigate the effect of oxygen concentration on denitrification. *Soil Biol. Biochem.* **1984**, *16* (4), 331−334.
(46) Bollman, A.; Conrad, R. Influence of O_2 availability on NO and N_2O release by nitrification and denitrification in soils. *Global Change Biol.* **1998**, *4* (4), 387−396.
(47) Strong, D. T.; Fillery, I. R. P. Denitrification response to nitrate concentrations in sandy soils. *Soil Biol. Biochem.* **2002**, *34* (7), 945−954.
(48) Rachhpal-Singh,; Nye, P. H. A model of ammonia volatilization from applied urea, I. development of the model. *Soil Sci.* **1986**, *37,* 9−20.
(49) Sposito, G. *The Chemistry of Soils;* Oxford University Press Inc.: New York, 1989.
(50) Master, Y. Transformations and Gasous Losses of N from Effluent Irrigated Soils. Master's thesis, Technion−Israel Institute of Technology, 2002.
(51) Kremen, A. Simulation of Nitrogen Transformations in Effluent Irrigated, Aggregated Soil. Ph.D. thesis, Technion−Israel Institute of Technology, 2004.
(52) McConnaughey, P. K.; Bouldin, D. R. Transient macrosite models of denitrification: II. Model results. *Soil Sci. Soc. Am. J.* **1985**, *49,* 891−895.
(53) Betlach, M. R.; Tiedje, J. M. Kinetic explanation for accumulation of nitrite, nitric oxide and nitrous oxide during bacterial denitrification. *Appl. Environ. Microbiol.* **1981**, *42* (6), 1074−1084.
(54) Alleman, J. E. Elevated nitrite occurrence in biological wastewater treatment systems. *Water Sci. Technol.* **1984**, *17,* 409−419.
(55) Suthersan, S.; Ganczarczyk, J. J. Inhibition of nitrite oxidation during nitrification−some observations. *Water Pollut. Res. J. Can.* **1986**, *21,* 257−266.
(56) Burns, L. C.; Stevens, R. J.; Laughlin, R. J. Production of nitrite in soil by simultaneous nitrification and denitrification. *Soil Biol. Biochem.* **1996**, *28* (4/5), 609−616.
(57) Mosier, A.; et al. Closing the global N_2O budget: Nitrous oxide emissions through the agricultural nitrogen cycle. *Nutr. Cycling Agroecosyst.* **1996**, *50,* 225−248.
(58) Stevens, R. J.; Laughlin, R. J.; Malone, J. P. Measuring the mole fraction and source of nitrous oxide in the field. *Soil Biol. Biochem.* **1998**, *30* (4), 541−543.
(59) Müller, C.; Abbasi, M. K.; Kammann, C.; Clough, T. J.; Sherlock, R. R.; Stevens, R. J.; Jäger, H.-J. Soil respiratory quotient determined via barometric process separation combined with nitrogen-15 labeling. *Soil Sci. Soc. Am. J.* **2004**, *68,* 1610−1615.
(60) Schramm, A. In situ analysis of structure and activity of the nitrifying community in biofilms, aggregates, and sediments. *Geomicrobiol. J.* **2003**, *20* (4), 313−333.
(61) Chenu, C.; Hassinek, J.; Bloem, J. Short-term changes in the spatial distribution of microorganisms in soil aggregates as affected by glucose addition. *Biol. Fertil. Soils* **2001**, *34,* 349−356.

Received for review October 30, 2004. Revised manuscript received March 28, 2005. Accepted March 31, 2005.

ES048304Z